Electronic Supplementary Material (ESI) for Analyst.

Multi-scene visual hydrazine hydrate detection based on dibenzothiazole derivative

Yingshuang Chen, Chuanfeng Zhao, Xinyi Liu, Qian Zhang, Yuliang Jiang*, Jian Shen*

Jiangsu Collaborat Innovat Ctr Biomed Funct Mat, Jiangsu Key Lab Biofunct Mat, Sch Chem & Mat Sci, Nanjing Normal University, Nanjing 210023, Jiangsu, PR China

List of contents

1. Experimental section

1.1 Materials and apparatus

All chemicals, including reactants, catalysts and solvents were purchased from commercial suppliers and used without further purification unless otherwise stated. The ^{1}H NMR and ^{13}C NMR spectra were obtained on an AVANCE III HD AN-400 MHz spectrometer (Bruker, Germany). Mass spectroscopy (MS) was recorded on a LCMS-2020 spectrometer (Shimadzu, Japan). Infrared data was obtained from ALPHA II (Bruker, Germany). Ultraviolet-Visible (UV-vis) absorption studies were acquired with a Lambda 650s spectrophotometer (PerkinElmer, USA) and the fluorescence spectrum of probe were carried out on an F-7100 fluorescence spectrophotometer (Hitachi, Japan). Fluorescence imaging experiments of cells and zebrafish were conducted using an A1 confocal laser scanning microscope (Nikon, Japan).

1.2 Synthesis of compound 1

2-aminophenthiol (2 mmol, 0.25 g), 4-bromo-2-hydroxybenzaldehyde (2 mmol, 0.40 g), absolute ethanol (15 mL), H_2O_2 (30%, 12.0 mmol, 1.20 mL) and HCl (37%, 8.5mmol, 0.70mL) were added into a 100 mL three-neck flask in turn, and the white solid appeared after stirring for about 2 min at room temperature. The reaction process was monitored by TLC until the end, the product was filtered and washed with absolute ethanol, then dried in vacuum to obtain white flocculent solid 0.50 g (81.7% yield). The chemical structures of compound 1 were characterized by ^{1}H NMR (Fig. S1).^{1}H NMR (400 MHz, DMSO-d6) δ 11.71 (s, 1H), 8.39 (d, J = 2.5 Hz, 1H), 8.21 - 7.93 (m, 2H), 7.67 - 7.35 (m, 3H), 7.06 (d, J = 8.8 Hz, 1H).

1.3 Synthesis of Compound 2

Compound 1 (2 mmol, 0.61g) and 4-formylphenylboric acid (3 mmol, 0.51g), $Pd(PPh_3)_4$ (0.25 mmol, 0.06 g) were added into a 100 mL three neck flask, then added toluene (20 mL) and K_2CO_3 (6 mmol, 0.833g, dissolved in 3 ml of water), the mixture was heated to 120℃ for 24 h under nitrogen protection, the reaction process was monitored by TLC until the end. Cooled to room temperature, then remove the solvent under reduced pressure. The crude product was separated by column chromatography (ethyl acetate: petroleum ether =1:15) and vacuum dried to obtain

yellow solid 0.41g (61.9% yield). The chemical structures of compound 2 were characterized by ^{1}H NMR and ^{13}C NMR (Fig.S2-S3). ^{1}H NMR (400 MHz, DMSO-d6) δ 11.84 (s, 1H), 10.08 (dd, J = 10.6, 1.7 Hz, 1H), 8.61 (t, J = 2.1 Hz, 1H), 8.17 (d, J = 7.9 Hz, 1H), 8.12 (d, J = 8.1 Hz, 1H), 8.08-7.92 (m, 4H), 7.86 (dt, J = 8.7, 2.1 Hz, 1H), 7.57 (t, J = 7.6 Hz, 1H), 7.47 (t, J = 7.5 Hz, 1H), 7.24 (dd, J = 8.6, 1.6 Hz, 1H); ^{13}C NMR (101 MHz, DMSO-d6) δ 193.18, 164.39, 157.16, 151.91, 145.58, 135.34, 135.19, 131.55, 130.81, 130.75, 130.69, 128.42, 127.29, 126.95, 125.58, 122.80, 122.50, 119.81, 118.26.

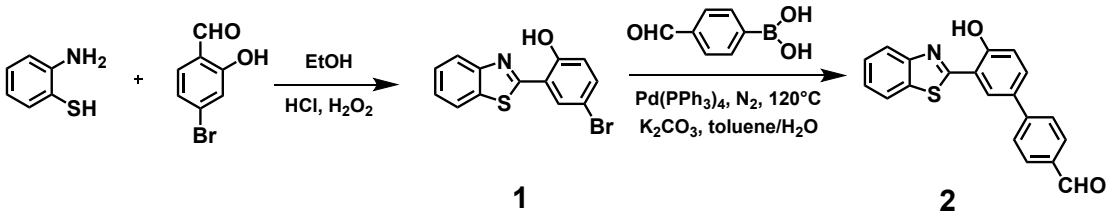

Scheme S1 The synthetic steps of compound 1 and 2.

2. ^{1}H NMR spectroscopy of compound 1

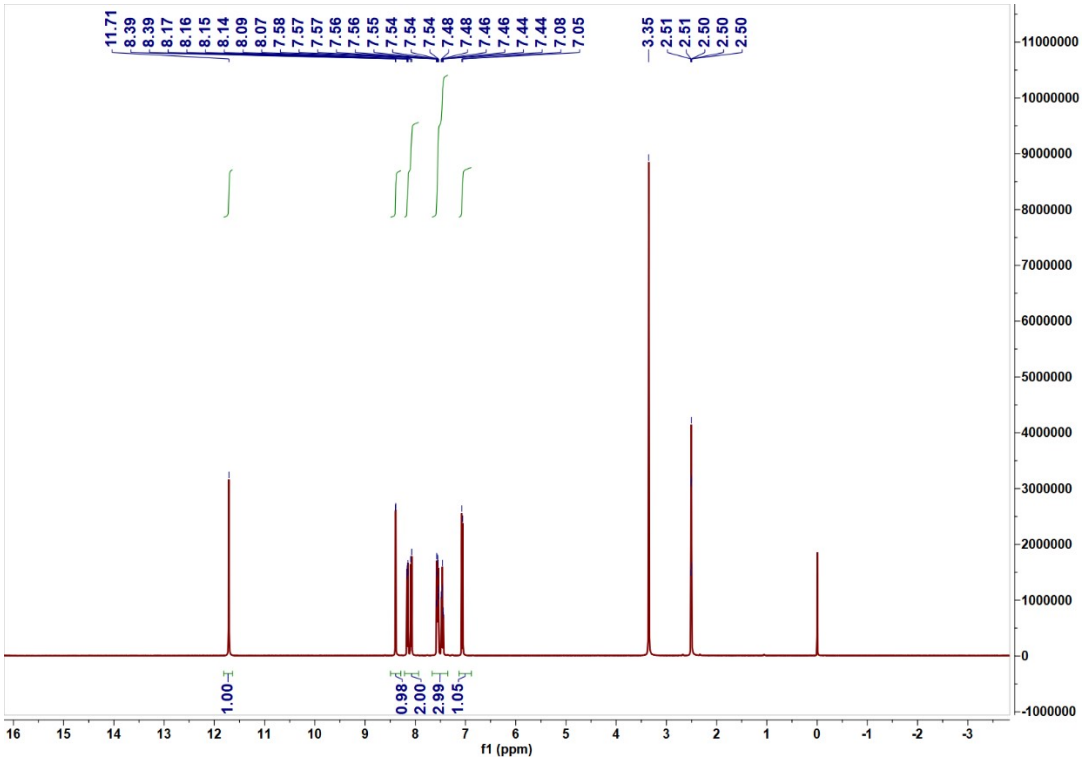

Fig. S1 ^{1}H NMR spectroscopy of compound 1.

3. ^{1}H NMR spectroscopy of compound 2

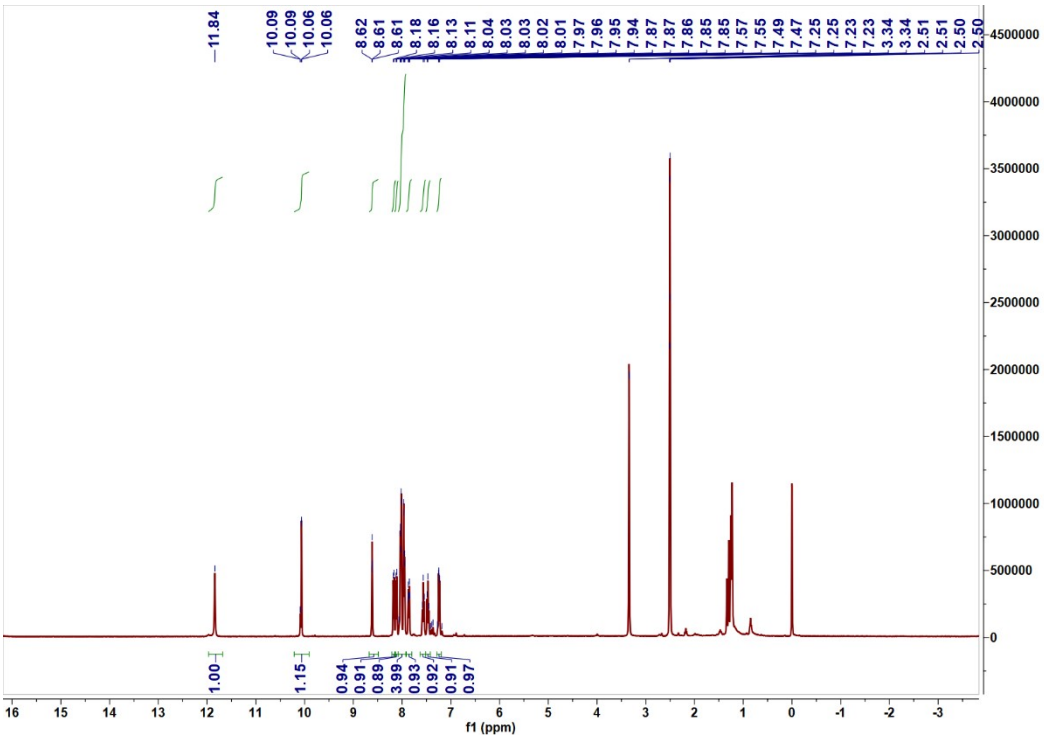

Fig. S2 ^{1}H NMR spectroscopy of compound 2.

4. ^{13}C NMR spectroscopy of compound 2

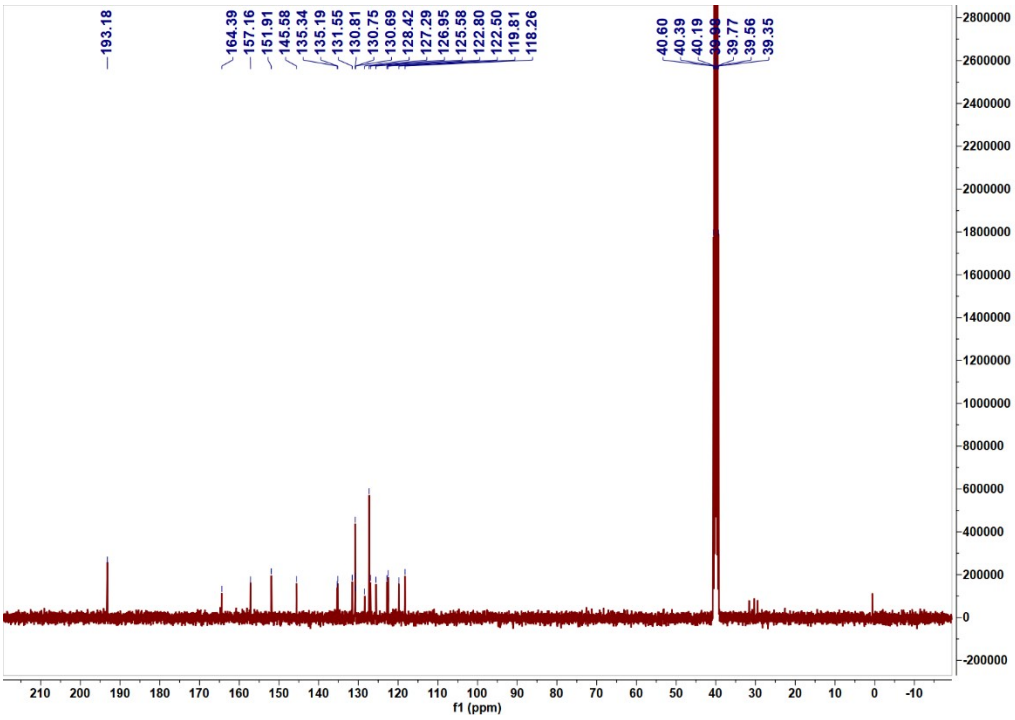

Fig. S3 ^{13}C NMR spectroscopy of compound 2.

5. ^{1}H NMR spectroscopy of probe DBTD

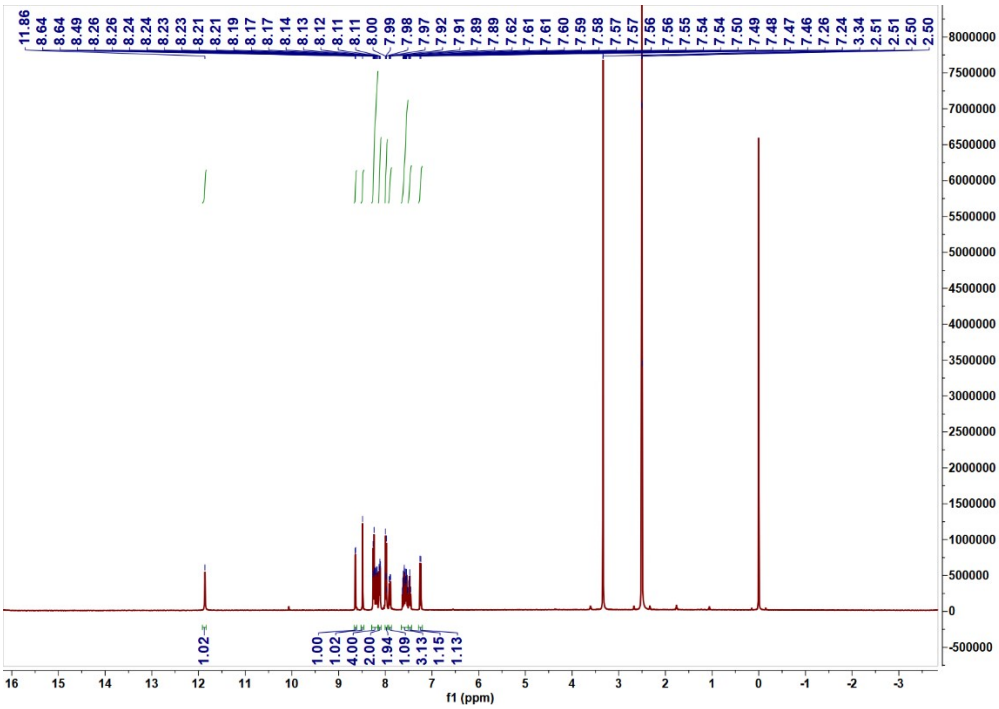

Fig. S4 ^{1}H NMR spectroscopy of probe DBTD.

6. ^{13}C NMR spectroscopy of probe DBTD

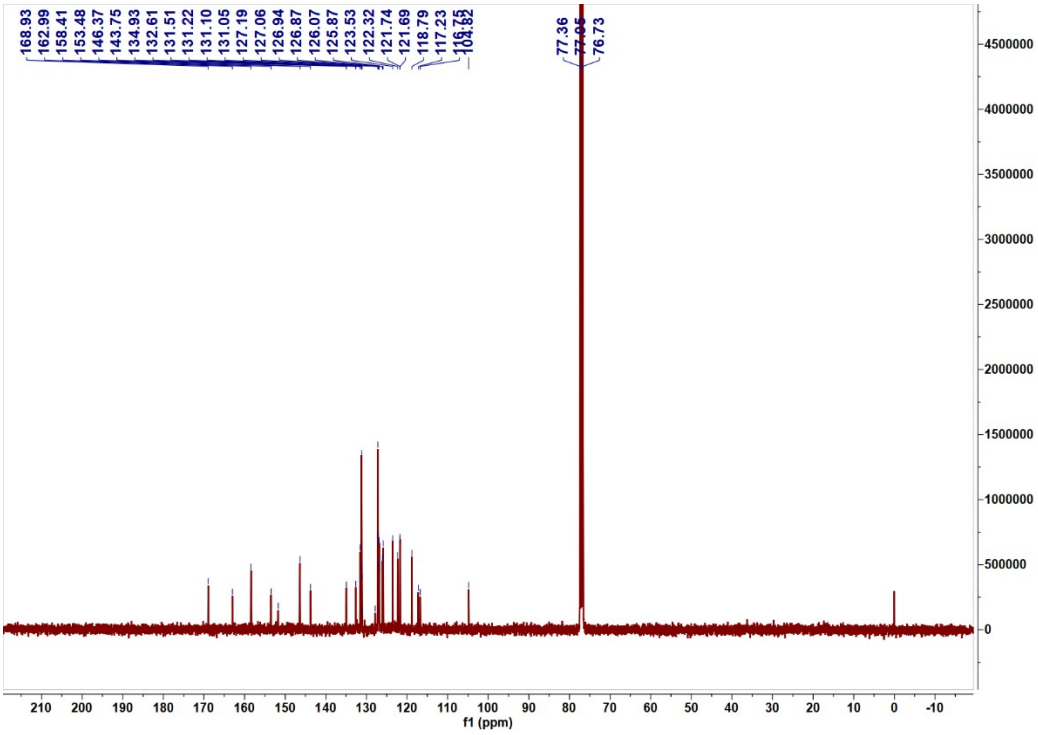

Fig. S5 ^{13}C NMR spectroscopy of probe DBTD.

7. MS spectroscopy of probe DBTD

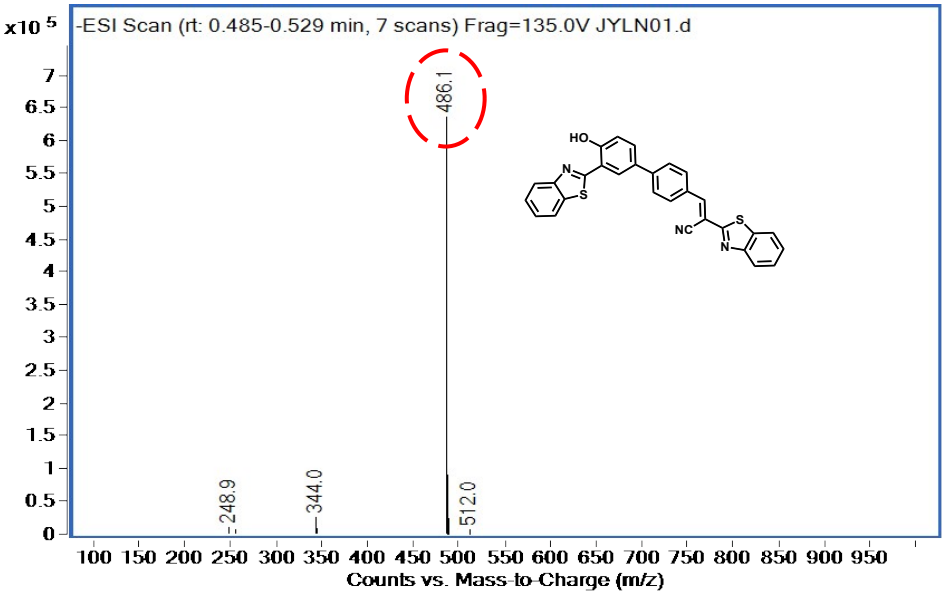

Fig. S6 MS spectroscopy of probe DBTD.

8. Table S1 Comparison of analytical performance of early N_2H_4 probes

Probes	Response mode	Limit of detection	Response time	Reference
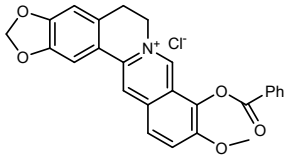	Turn off	1.37 μM	60 min	[1]
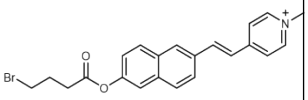	Ratiometric	2.6 μM	120 min	[2]
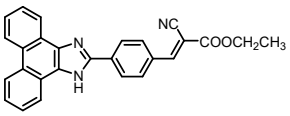	Ratiometric	1.6 μM	15 min	[3]
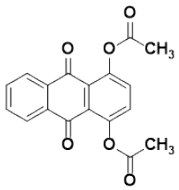	Turn on	----	60 min	[4]
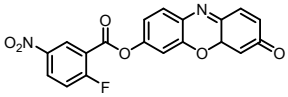	Turn on	0.84 μM	30 min	[5]
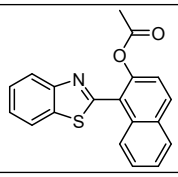	Turn on	0.49 μM	60 min	[6]

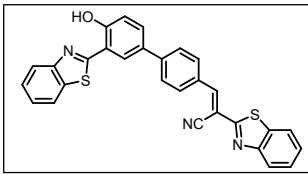	Ratiometric	0.438 μM	45 min	This Work

9. Table S2 the fluorescence quantum yield of probe DBTD in the absence or presence of N_2H_4

Compound	λ_{abs} /nm	λ_{em} /nm	Φ_F
DBTD	383/571	650	0.057
DBTD-N_2H_4	431/571	490	0.250

10. Fluorescence response of probe DBTD to different analytes

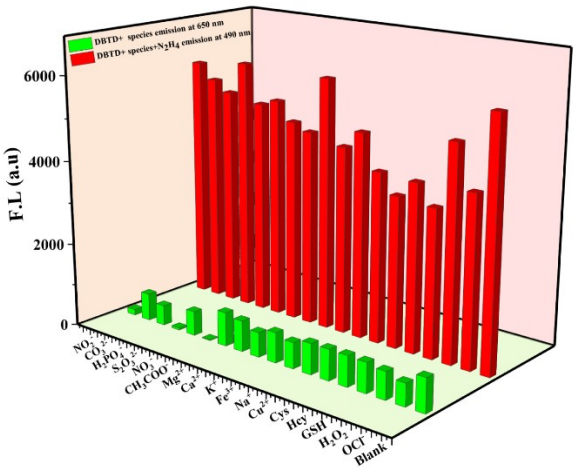

Fig. S7 (a) Fluorescence responses of probe DBTD (10 μM) treated with 260 μM other various competitive species (NO_2^-, NO_3^-, CH_3COO^-, CO_3^{2-}, $H_2PO_4^-$, $S_2O_3^{2-}$, Ag^+, K^+, Cu^{2+}, Ca^{2+}, Fe^{3+}, Na^+, Mg^{2+}, OCl^-, Cys, Hcy, GSH, H_2O_2) and N_2H_4 (130 μM) at room temperature for 40 min: λex = 369 nm. Slit width: 5 nm / 5 nm.

11. ^{1}H NMR titration in DMSO-d6 solution

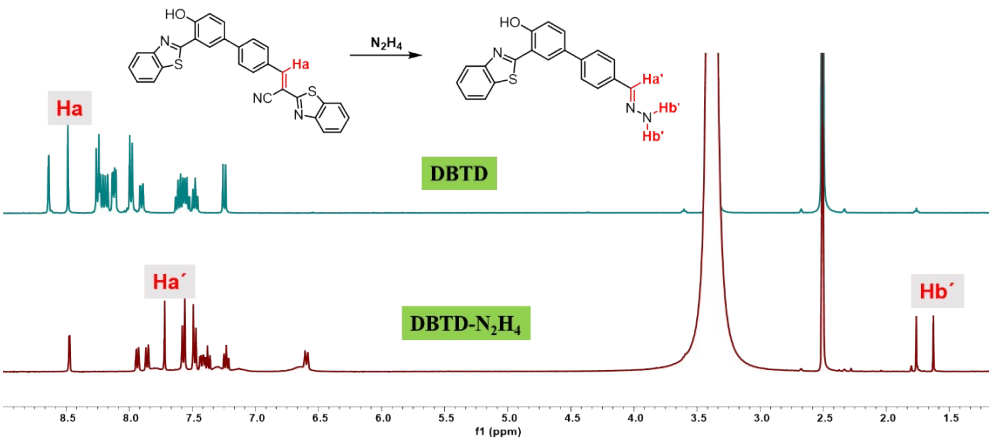

Fig. S8 ^{1}H NMR titration in DMSO-d6 solution.

12. FT-IR of the probe DBTD and the adduct DBTD-N_2H_4

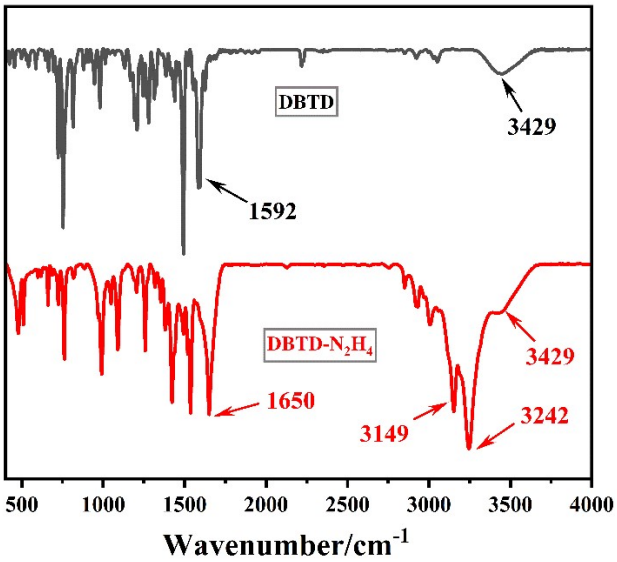

Fig. S9 FT-IR of the probe DBTD and the adduct DBTD-N_2H_4.

13. MS spectroscopy of the DBTD-N_2H_4

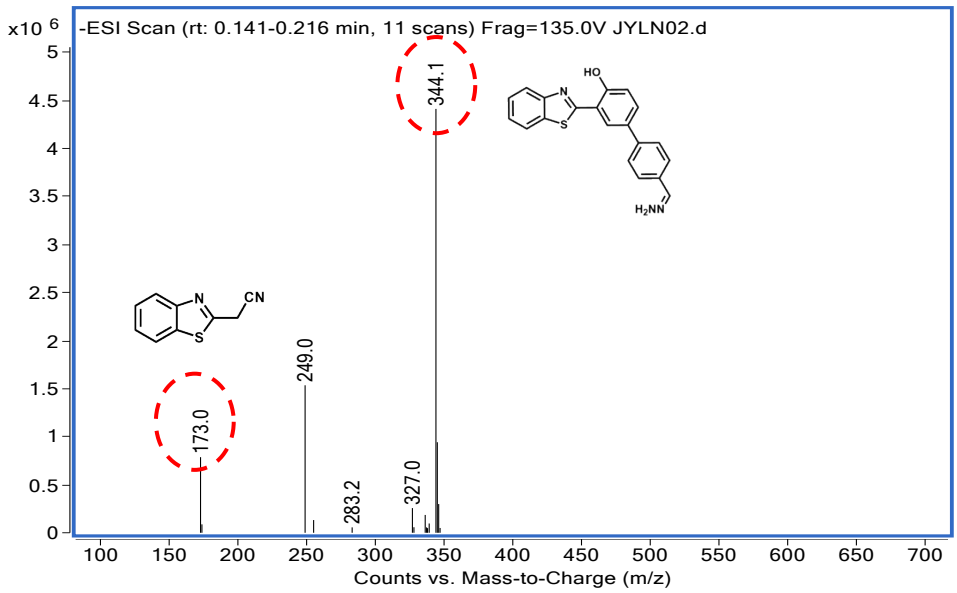

Fig. S10 MS spectroscopy of the DBTD-N_2H_4.

14. The linear relationship of the fluorescence intensity of probe DBTD with the concentration of N_2H_4 in two kinds of water samples

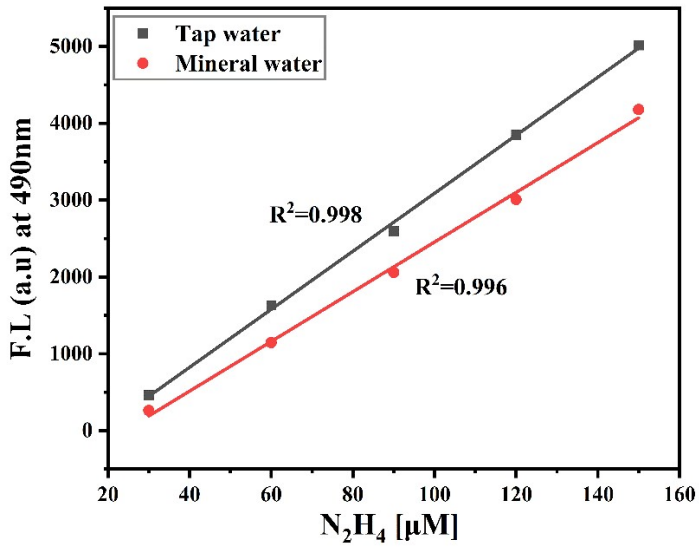

Fig. S11 The linear relationship of the fluorescence intensity of probe DBTD at 490 nm with the concentration of N_2H_4 (30 μM - 150 μM) in the tap water and mineral water at room temperature. λex = 369 nm. Slit width: 5 nm / 5 nm.

15. The cells cytotoxicity of probe DBTD

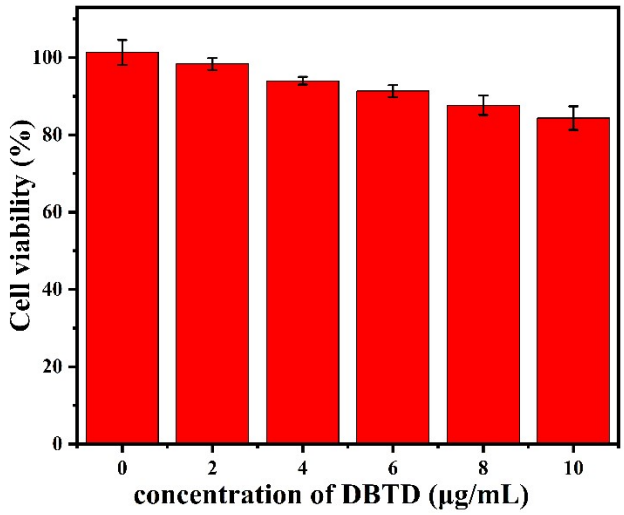

Fig. S12 Cytotoxicity of probe DBTD by a MTT assay (n = 3).

16. Intracellular co-localization fluorescence imaging of the DBTD-N_2H_4

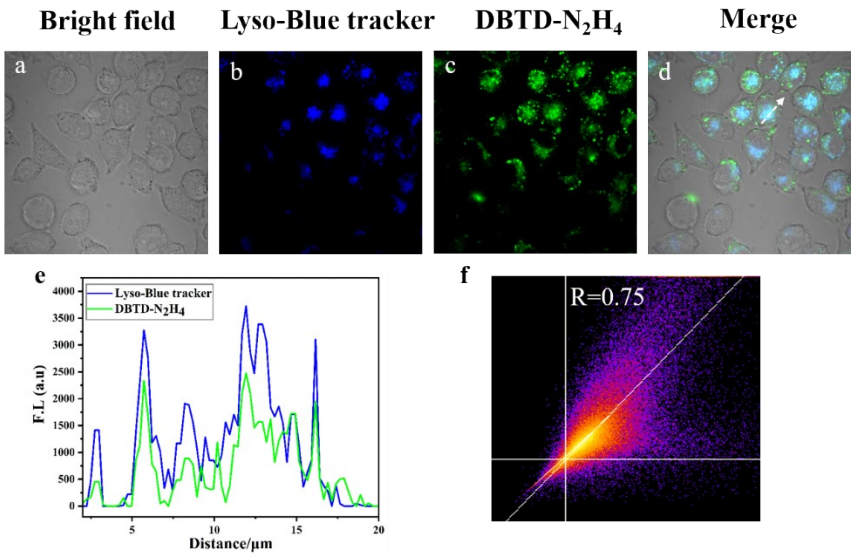

Fig. S13 Intracellular co-localization fluorescence imaging of the DBTD-N_2H_4 (10 μM). (a) Bright field. (b) Lyso-Blue tracker (100 nM). (c) Confocal fluorescence images of the DBTD-N_2H_4 on the green channel. (d) Merged image of a, b and c. (e) Fluorescence intensity profiles in linear regions of Hela cells (blue for Lyso-Blue tracker; Green for DBTD-N_2H_4). (f) Colocalization scatterplots of (e). PC: 0.75. Blue channel: λex = 405 nm, λem = 425 - 475nm; Green channel: λex = 488 nm, λem = 500 - 550 nm; Scale bar = 20 μm.

References

1.S. T. Ruan, Y. Gao, Y. Y. Wang, M. X. Li, H. Y. Yang, J. Song, Z. L. Wang and S. F. Wang, New J. Chem., 2020, **44**, 15752.

2. J. L. Han, X. X. Yue, J. P. Wang, Y. Zhang, B. H. Wang and X. Z. Song, Chinese Chem Lett., 2020, **31**, 1508-1510.

3. Z. X. Li, W. Y. Zhang, C. X. Liu, M. M. Yu, H. Y. Zhang, L. Guo and L. H. Wei, Sens. Actuators, B., 2017, **241**, 665-671.

4. S. Sinha, P. G, Sagarika Dev, S. Mukhopadhyay, T. Mukherjee and S. Ghosh, Sens. Actuators, B., 2015, **221**, 418-426.

5. T. Tang, Y. Q. Chen, B. S. Fu, Z. Y. He, H. Xiao, F. Wu, J. Q. Wang, S. R. Wang and X. Zhou, Chinese Chem Lett., 2016, **27**, 540-544.
6. C. T. Liu, F. Wang, T. Xiao, B. Chi, Y. H Wu, D. R. Zhu and X. Q. Chen, Sens. Actuators, B., 2018, **256**, 55-62.